Pressure Drop Measurements in the Transition Region for a Circular Tube with Three Different Inlet Configurations

Afshin J. Ghajar

Khushrow F. Madon*

School of Mechanical and Aerospace Engineering, Oklahoma State University, Stillwater, Oklahoma

■ Pressure drop measurements were made in a horizontal circular straight tube with reentrant, square-edged, and bell-mouth inlets under isothermal flow conditions. The experiments covered a Reynolds number range from about 500 to 15,000. The fully developed skin friction coefficients for the three inlet configurations showed that the range of Reynolds number values for which transition flow exists is 1980–2600 for the reentrant inlet, 2070–2840 for the square-edged inlet, and 2125–3200 for the bell-mouth inlet. A correlation for prediction of the fully developed skin friction coefficient in the transition region for each inlet is recommended. In the entrance region, qualitative results are presented for the variation of laminar apparent friction factor with tube length for different inlets. Available friction factor correlations in the laminar entrance and fully developed transition regions are compared with our experimental data for different inlets.

Keywords: *pressure drop, transition region, friction factor, circular tube, heat exchangers*

INTRODUCTION

An important design problem in industrial heat exchangers arises when flow inside the tubes falls into the transition region. In practical engineering design, the usual recommendation is to avoid design and operation in this regime; however, this is not always feasible under design constraints. The usually cited transition Reynolds number of about 2100 applies, strictly speaking, to a very steady and uniform entry flow with a rounded entrance. If the flow has a disturbed entrance typical of heat exchangers, in which there is a sudden contraction and possibly even a reentrant entrance, the transition Reynolds number will be different.

Numerous experimental, analytical, and numerical studies are available for pressure drop in horizontal tubes with a rounded entrance in the laminar, transitional, and turbulent flow regimes. These works have been reviewed by Shah and Johnson [1] and Kakac et al [2]. However, very little information that is of immediate use to a design engineer (ie, correlation) is available to predict the fully developed transitional skin friction coefficient in a tube with a disturbed entrance.

The results of some studies in the entrance and fully developed regions of a circular horizontal pipe with a rounded entrance for all three flow regimes are presented in the form of friction factor correlations (empirical or numerical) in Table 1. The type of inlet configuration influences the development of friction factor along the pipe and the beginning and end of the transition region. Therefore, the application of these correlations to tubes with disturbed entrances should be investigated.

The purpose of this study was to create an accurate and broad pressure drop (friction factor) database across all flow regimes in the entrance and fully developed regions of a horizontal pipe fitted with three different inlet configurations (reentrant, square-edged, and bell-mouth). The database was used to investigate the influence of inlet configuration on the start and end of the fully developed transition region for each inlet and the development of an appropriate empirical friction factor correlation in the fully developed transition region for each inlet. In addition, the database was used to establish the validity of the correlations presented in Table 1 for various inlet configurations.

FRICTION FACTOR TERMINOLOGY

In this study, when reporting the pressure drop in terms of friction factor, the terms *skin friction coefficient* and *apparent friction factor* are used. The skin friction coefficient, denoted by c_f, refers to a fully developed friction factor that considers pressure drop arising only from shear stresses at the wall. The apparent friction factor, denoted by f_{app}, refers to the entrance region friction factor, which considers pressure drop arising from both momentum flux during the velocity profile development and the shear stresses at the wall. Obviously, the apparent friction factor is always greater

*Present address: Muskegon Piston Ring Co., Manitowoc, MI 54221.

Address correspondence to Professor A. J. Ghajar, School of Mechanical and Aerospace Engineering, Oklahoma State University, Stillwater, OK 74078.

Experimental Thermal and Fluid Science 1992; 5:129–135

0894-1777/92/$3.50

Table 1. Friction Factor Correlations for a Smooth Circular Duct

Investigator	*Correlation*	*Recommended Re Range*
Shah[16]	$f_{app} = \frac{1}{Re}\left(\frac{3.44}{\zeta^{1/2}} + \frac{0.31/\zeta + 16 - 3.44/\zeta^{1/2}}{1 + 0.00021/\zeta^2}\right)$, where $\zeta = (x/D)/\mathrm{Re}$	Laminar
Churchill [14]	$\frac{2}{c_f} = \left\{\frac{1}{\left[(8/Re)^{10} + (Re/36{,}500)^{20}\right]^{1/2}} + \left[2.21\, ln\left(\frac{Re}{7}\right)\right]^{10}\right\}^{1/5}$	Laminar, transition, and turbulent
Hrycak and Andruskhiw [13]	$c_f = -3.10 \times 10^{-3} + 7.125 \times 10^{-6}\,\mathrm{Re} - 9.70 \times 10^{-10}\,\mathrm{Re}^2$	2100–4500
Bhatti and Shah [15]	$c_f = A + B/\mathrm{Re}^{1/m}$, where $A = 0$, $B = 16$, $m = 1$ for $\mathrm{Re} < 2100$; $A = 0.0054$, $B = 2.3 \times 10^{-8}$, $m = -2/3$ for $2100 < \mathrm{Re} \leq 4000$; $A = 1.28 \times 10^{-3}$, $B = 0.1143$, $m = 3.2154$ for $\mathrm{Re} > 4000$	Laminar, transition, and turbulent
Blasius [10]	$c_f = 0.0791\,\mathrm{Re}^{-0.25}$	4×10^3 to 10^5

than the skin friction factor, and they both approach asymptotically their fully developed values. In the fully developed region the local apparent friction factor equals the local skin friction coefficient.

EXPERIMENTS

A schematic diagram of the overall experimental setup used for pressure drop experiments is shown in Fig. 1. The experimental setup shown was also used for heat transfer [3, 4] and intermittency factor [5] measurements. The pressure drop test section is a horizontal seamless 316 stainless steel circular tube with an inside diameter of 1.58 cm and an outside diameter of 1.91 cm. The total length of the test section is 6.10 m, providing a maximum length-to-diameter ratio (L/D) of 386. The test section was insulated from the environment by using fiberglass pipe insulation and vapor proof pipe tape. The total thickness of the insulation materials is about 3.18 cm. To ensure a uniform fluid bulk temperature at the exit of the test section, a mixing well that consisted of several baffles was used. A one-shell and two-tube pass heat exchanger was used to cool the fluid from the test section to a desirable inlet bulk temperature.

Provision was also made to heat the pressure drop test section by the passage of high-amperage, low-voltage dc current in order to study the influence of heating on pressure drop measurements. For this purpose, copper plates were silver-arc soldered to the ends of the test section to secure a well-defined electric circuit through the end plates, and thermocouples were attached to selected locations on the pressure drop test section. However, for this study experiments were conducted under isothermal flow conditions.

For pressure drop measurements, pressure taps were placed at the top on the outer surface of the wall at close intervals near the entrance and at greater intervals further downstream (see Fig. 2 for details). Twenty-one pressure tap stations were designated with one 0.198 cm diameter hole drilled at each station. Each of the pressure tap holes was deburred with a special tool to ensure the characteristics of a smooth tube. Pressure measurements were made with three Dwyer differential pressure gauges with ranges of 0–1 in. H_2O, 0–5 in. H_2O, and 0–20 in. H_2O and one 0–20 in. mercury manometer. The differential pressure gauges had an accuracy of ±3% reading, and their calibration was checked regularly during the experiments. To enable us to take sequential pressure drop measurements along the test section, a pressure tap manifold was constructed [6]. This manifold made it possible to measure pressure drop from the reference pressure tap to any of the other 20 pressure taps.

To ensure a uniform velocity distribution in the test fluid before it entered the test section, the flow passed through a calming and inlet section (see Fig. 3). The calming section consisted of a 17.8 cm diameter acrylic plastic cylinder with three perforated acrylic plastic plates with an open area ratio of 0.312 (73 holes per plate, hole diameter 1.1 cm) followed by tightly packed soda straws (inside diameter 0.57 cm, length 10.2 cm, open area ratio 0.915) sandwiched between galvanized steel mesh screens (wire diameter 0.07 cm, mesh width 0.28 cm, open area ratio 0.597). Before leaving the calming section test fluid passed through a fine mesh screen (wire diameter 0.03 cm, mesh width 0.14 cm, open area ratio 0.692). The total length of the calming section was 61.6 cm. Test fluid leaving the calming section entered the inlet section and flowed undisturbed through 23.5 cm of a 16.5 cm diameter acrylic plastic tube before it entered the test section. This was done to ensure a uniform velocity distribution upon entering the test section. The calming and inlet sections were also equipped with air bleed valves that were used to evacuate air during startup.

The inlet section has the versatility of being modified to incorporate a reentrant or a bell-mouth entrance (see Fig. 3). The reentrant entrance was simulated by sliding 1.91 cm of the tube entrance length into the inlet section (Fig. 3), which was otherwise the square-edged (sudden contraction) entrance. For the bell-mouth entrance, a nozzle had to be constructed to replace the inlet section of Fig. 3. The nozzle was designed according to the method suggested by Morel [7] and was constructed of fiberglass. The nozzle has a contraction ratio of 10.7 and a total length of 23.6 cm. Construction of the nozzle, a multistep process, consisted of constructing a two-dimensional contour on a numerically controlled milling machine from a computer-generated profile, using the contour and a hydraulic follower on a lathe to produce an axisymmetric male mold, and forming the fiberglass nozzle around the male mold, with aluminum flanges formed in.

The inlet and exit bulk temperatures were measured by

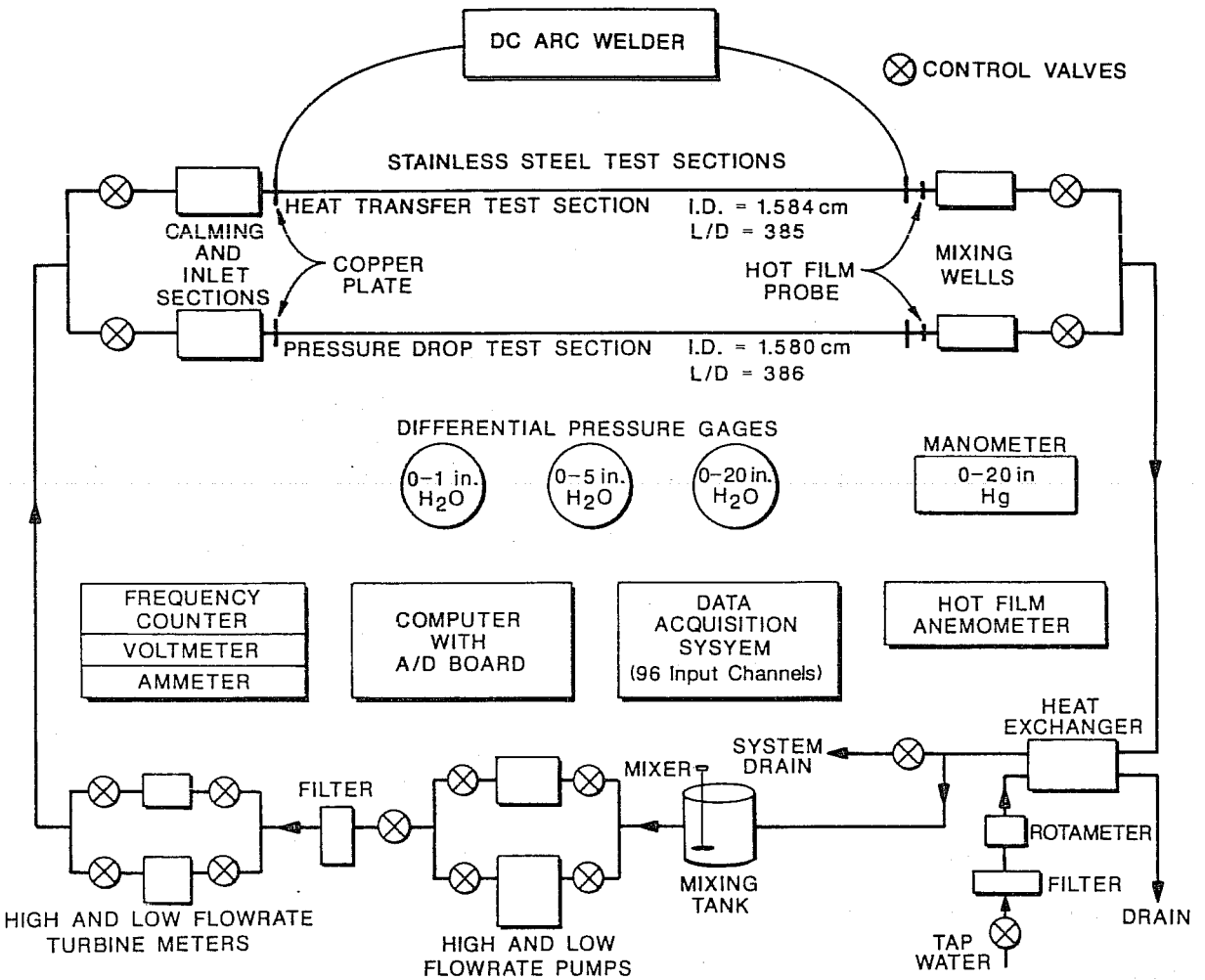

Figure 1. Schematic of the experimental setup.

means of a calibrated thermocouple probe (copper-constantan T-type) inserted in the calming section and the mixing well, respectively. Calibration of thermocouple probes showed that they were accurate within $\pm 0.4°C$. The data acquisition system used for the temperature measurements consisted of a Cole-Parmer MAC-14 datalogger with 96 input channels interfaced with a personal computer. Isothermal flow conditions were ensured when the inlet and outlet bulk temperatures were nearly equal (within 0.2°C of each other). The flow rate was measured by a calibrated turbine meter located upstream from the test section. The turbine meter had a linearity of $+0.5\%$ of reading and a repeatability of less than $+0.10\%$ of reading.

To prevent the pumps from transmitting noise and vibration through the experimental setup, they were mounted inside a plywood box lined with insulation. In addition, rubber hoses were connected to the pump box to prevent vibration transmission to the fluid return tubing. All equipment was placed on damping pads to prevent transmission of vibration through the floor.

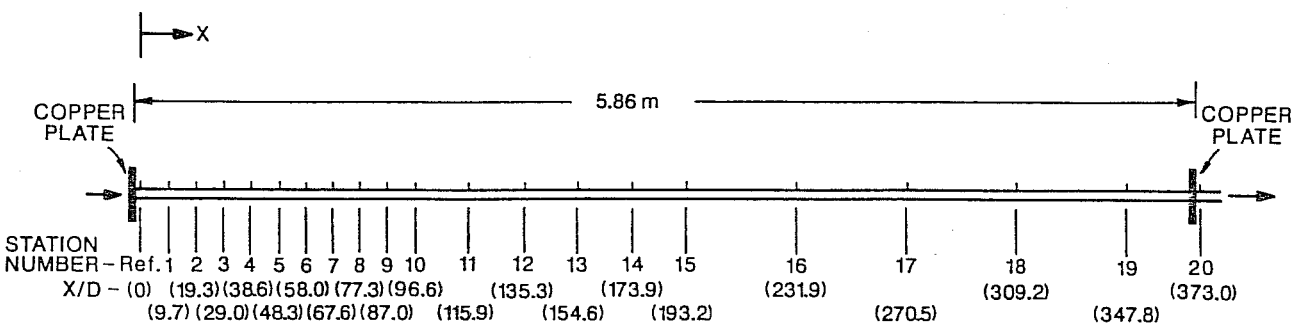

Figure 2. Pressure drop test section pressure tap distribution.

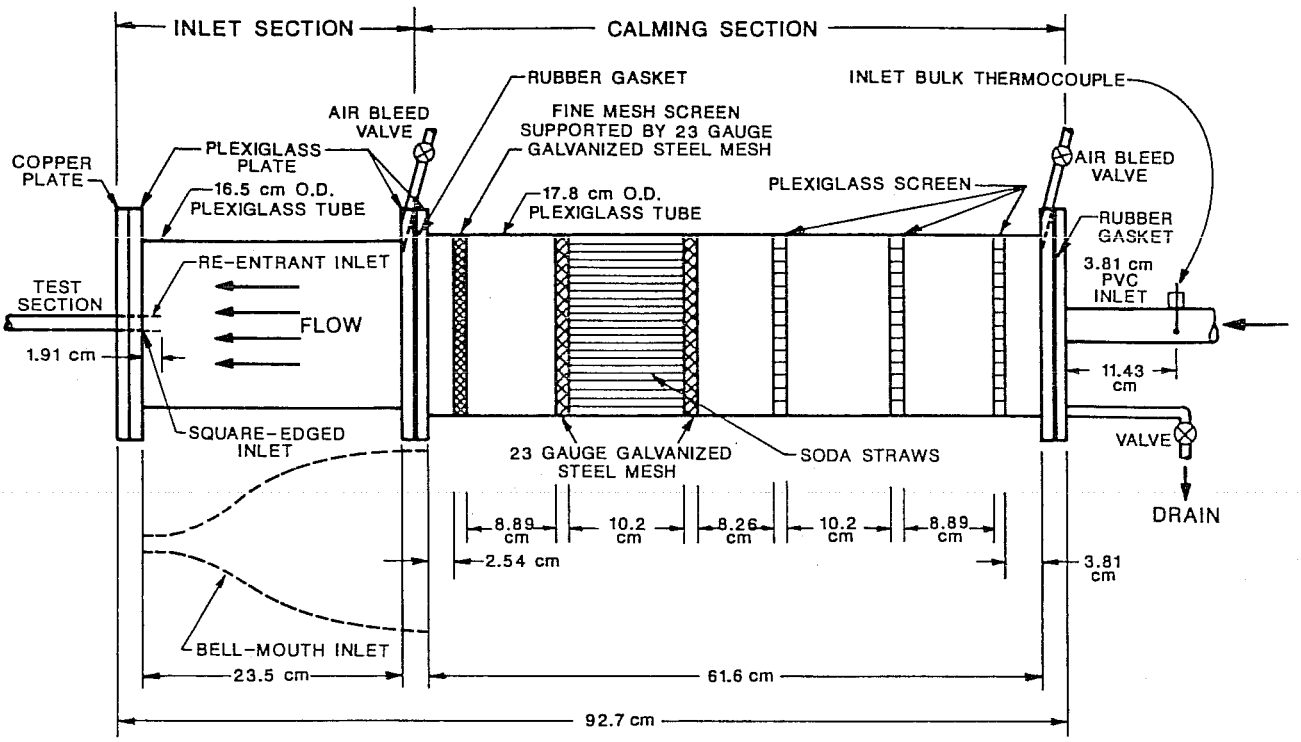

Figure 3. Schematic of the calming and inlet sections.

To develop the complement of experimental data (total of 114 runs), two test fluids were used in different concentrations. Full-strength concentrations of distilled water and ethylene glycol were followed by 61% and 70% mixtures of ethylene glycol (mass fraction), which gave local bulk Reynolds number ranging from about 500 to 15,000. The pressure drop measurements under isothermal flow conditions were carried out by measuring the pressure drop between the reference pressure tap and the other 20 pressure taps along the axis of the tube (see Fig. 2). In addition, inlet and outlet bulk temperatures and flow rate were measured. Using this information, the friction factor in the entrance region (apparent friction factor, f_{app}) and the fully developed region (skin friction coefficient, c_f) was calculated for all Reynolds numbers of interest. The physical properties needed for these calculations were those presented by Bohn et al [8] (also see Ref. 9).

The reliability of the flow circulation system and the experimental procedures were checked by making several calibration runs with distilled water and full-strength ethylene glycol, and results were compared with well-established friction factor correlation of Blasius [10] (see Table 1) for fully developed turbulent pipe flow and the fully developed laminar flow equation ($c_f = 16/\mathrm{Re}$). The experimental data were within $\pm 5.0\%$ of the predicted values. The uncertainty analysis of the overall experimental procedures using the method of Kline and McClintock [11] showed that there is a maximum of 5.2% uncertainty for friction factor calculations and maximum of 0.5% uncertainty for Reynolds number calculations. More detailed description of the experimental apparatus and procedures may be found in Refs. 6 and 12.

LAMINAR-TRANSITION-TURBULENT PRESSURE DROP MEASUREMENTS

To accurately define the fully developed transition region for the different inlets, only pressure drop measurements in the fully developed region ($x/D > 309$) were considered. Measurements in the entrance region for transitional flow Reynolds numbers were beyond the scope of this study. To obtain an accurate measurement of the fully developed pressure drop at the location of interest, four pressure drop measurements at each location were obtained and averaged. The averaged value of pressure drop was then used to calculate the fully developed skin friction coefficient. Figure 4 is a plot of fully developed skin friction coefficient versus Reynolds number for all flow regimes. From this figure the limits for the transition range for each inlet can be summarized as

Reentrant	$1980 < \mathrm{Re} < 2600$
Square-edged	$2070 < \mathrm{Re} < 2840$
Bell-mouth	$2125 < \mathrm{Re} < 3200$

Figure 4 shows that the data follow the laminar skin friction coefficient line closely (within $\pm 5\%$) up to Reynolds number of slightly greater than 1980–2125 (depending on the inlet type). At this point the onset of transition is seen to occur. The fully developed skin friction coefficients begin to increase in a parabolic manner until they reach the turbulent skin friction coefficient line. At Reynolds numbers greater than 2600–3200 (depending on the inlet type) the data begin to closely (within $\pm 5\%$) follow the turbulent skin friction coefficient line. The percent deviation of the experimental

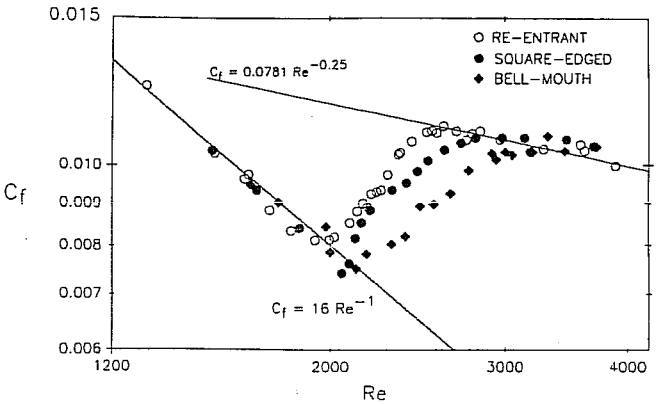

Figure 4. Fully developed skin friction coefficients for all flow regimes.

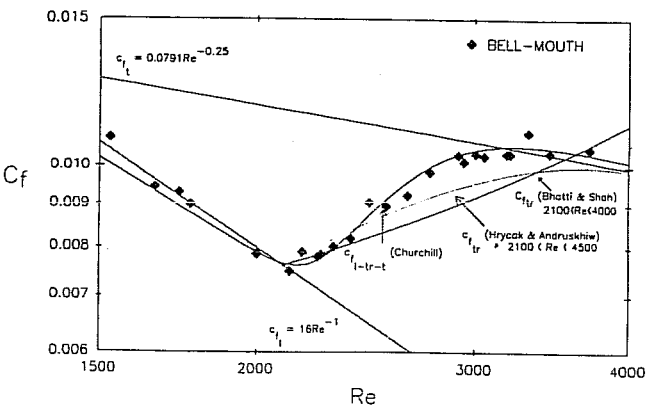

Figure 5. Comparison between experimental fully developed skin friction coefficients with a bell-mouth entrance and transition region friction factor correlations.

data in the laminar and turbulent regions from the established laminar ($c_f = 16/\mathrm{Re}$) and turbulent (Blasius [10] correlation, see Table 1) skin friction coefficient correlations were within $\pm 5.0\%$. This range is within the accuracy of the experimental data.

The results presented in Fig. 4 clearly establish the influence of the inlet configuration on the start and end of transition. As indicated, the inlet that caused the most disturbance (reentrant) produced an early transition (Re = 1980), and the inlet with least disturbance (bell-mouth) did not go into transition below a Reynolds number of about 2125. The square-edged inlet, which causes less disturbance than the reentrant inlet but more than the bell-mouth inlet, produced a transition Reynolds number of about 2070.

FULLY DEVELOPED TRANSITION REGION CORRELATIONS

Three of the available engineering correlations for computation of the fully developed skin friction coefficient in the transition region for a bell-mouth entrance are those of Hrycak and Andruskhiw [13], Churchill [14], and Bhatti and Shah [15] (see Table 1). No correlations were reported in the literature for other types of inlet configurations. Hrycak and Andruskhiw's [13] correlation is a second-order polynomial and predicts transition flow to begin at Re = 2100 and end at Re = 4500. The correlation proposed by Bhatti and Shah [15] gives a transition Reynolds number range between 2100 and 4000. Churchill's [14] correlation is based on a single model that continuously predicts fully developed skin friction coefficients in the laminar, transition, and turbulent flow regimes. The range of transition Reynolds number for his equation is between 2100 and 3200, which is in excellent agreement with our experimental findings. Figure 5 shows a comparison between our experimentally obtained fully developed skin friction coefficients in the transition region for a bell-mouth entrance and the predictions of these correlations. The agreement between our experimental data and Churchill's [14] continuous correlation is considered excellent. For the 17 data points shown in Fig. 5, the maximum absolute deviation between the experimental data and Churchill's correlation is 4.5%, and the majority of data points agree within $\pm 3\%$. These deviations are well within the uncertainty of our experimental measurements. The excellent agreement between our data and Churchill's [14] correlation also establishes the validity of our pressure drop measurements in the transition region.

For design purposes, simple correlations for prediction of the fully developed friction factor in the transition region for different inlets should be developed. As the data in the transition region appeared to be parabolic (see Hrycak and Andruskhiw [13]), they were fitted with a second-order polynomial using the least squares method. The resulting correlations, their limits, the number of points used, and the maximum and average absolute deviation from the fit for each inlet are listed below.

1. Reentrant

$$c_{f,\mathrm{tr}} = -9.88 \times 10^{-3} + 1.15 \times 10^{-5}\,\mathrm{Re} - 1.29 \times 10^{-9}\,\mathrm{Re}^2, \qquad 1950 < \mathrm{Re} < 2650$$

Max/avg abs. dev. % = 4.33/0.65; No. of points = 14

2. Square-edged

$$c_{f,\mathrm{tr}} = -2.56 \times 10^{-2} + 2.49 \times 10^{-5}\,\mathrm{Re} - 4.25 \times 10^{-9}\,\mathrm{Re}^2, \qquad 2055 < \mathrm{Re} < 3140$$

Max/avg abs. dev. % = 4.91/1.90; No. of points = 14

3. Bell-mouth

$$c_{f,\mathrm{tr}} = -8.03 \times 10^{-3} + 1.05 \times 10^{-5}\,\mathrm{Re} - 1.47 \times 10^{-9}\,\mathrm{Re}^2, \qquad 2075 < \mathrm{Re} < 3450$$

Max/avg abs. dev. % = 4.87/1.95; No. of points = 17

It is evident that the ranges specified for the above equations are broader than the actual limits for transitional behavior (see Fig. 4). It was desired that these equations should not predict an abrupt start and end of transition as shown by Hrycak and Andruskhiw's [13] and Bhatti and Shah's [15] equations but should show a gradual deviation, similar to Churchill's [14] correlation. For this reason the limits were stretched as much as possible into the laminar and turbulent regimes. The stretching imposed a limitation by way of an

increased absolute average and local deviations. These correlations predict, within the maximum local absolute deviations mentioned above for each case, the transitional as well as laminar and turbulent fully developed skin friction coefficients within the stretched limits. Outside the specified limits for each correlation, the established laminar ($c_f = 16/\mathrm{Re}$) and turbulent correlations (Blasius [10], see Table 1.) should be used.

LAMINAR APPARENT FRICTION FACTORS

To investigate the validity of Shah's [16] correlation presented in Table 1, pressure drop measurements over the entire length of the tube expressed as apparent friction factors for laminar flow are presented in this section. At each pressure tap location along the pipe (see Fig. 2), four pressure drop measurements were obtained and averaged. The averaged value of the pressure drop at each location was then used to calculate the apparent friction factor. It should be noted that as we approach the fully developed region, the local apparent friction factor equals the local skin friction factor.

Figures 6 and 7 display the laminar apparent friction factors for the two extreme inlets (reentrant and bell-mouth) in the form used by Langhaar [17], with the apparent friction factor multiplied by the Reynolds number versus the Reynolds number divided by the dimensionless axial location of the pressure taps (x/D). These figures also show the curve-fit expression for apparent friction factor suggested by Shah [16] and listed in Table 1. From Figs. 6 and 7 it can be observed that, for a particular inlet, the $f_{app}(\mathrm{Re})$ factor is not just a function of $\mathrm{Re}/(x/D)$ as predicted by Shah's [16] equation, but is a strong function of Reynolds number as well for $\mathrm{Re} < 1500$. For high laminar flow Reynolds numbers ($\mathrm{Re} > 1500$), the $f_{app}(\mathrm{Re})$ factor becomes an asymptotic function of $\mathrm{Re}/(x/D)$, and the friction factor curves become almost independent of Reynolds number. Similar behavior was observed for the square-edged inlet (see Refs. 6 and 18).

The results of Fig. 6 indicate that the correlation proposed by Shah [16] should not be used for the reentrant entrance. Similar results were observed for the square-edged entrance. However, Fig. 7 indicates that for Reynolds numbers greater than 1500 Shah's correlation predicts the bell-mouth laminar apparent friction factors very well. The accuracy of the correlation improves considerably for $x/D > 48$.

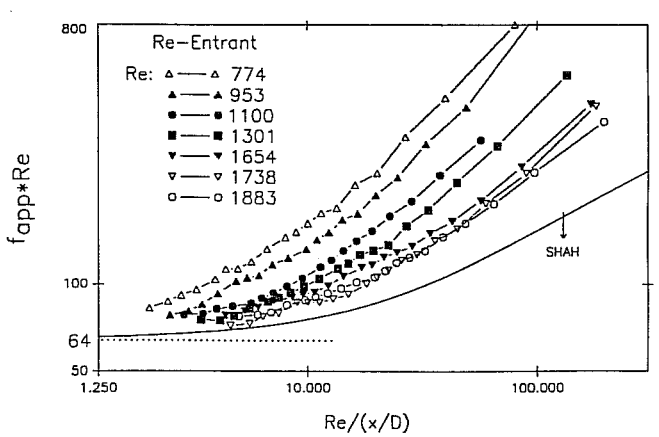

Figure 6. Comparison between experimental laminar flow apparent friction factors with reentrant entrance and correlation of Shah [16].

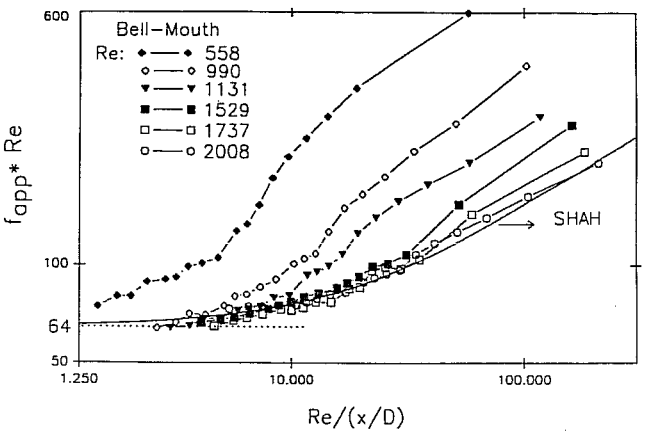

Figure 7. Comparison between experimental laminar flow apparent friction factors with bell-mouth entrance and correlation of Shah [16].

Another interesting observation from Figs. 6 and 7 is that, for a particular inlet, as the Reynolds number increases, the tube length required for the apparent friction factor to become constant decreases. For example, for the reentrant inlet (see Fig. 6) at $\mathrm{Re} = 774$, the apparent friction factor becomes constant after about 300 diameters from the inlet, and at $\mathrm{Re} = 1883$ the apparent friction factor becomes constant after about 200 diameters from the inlet. However, as the Reynolds number increases ($\mathrm{Re} > 1301$), the entrance length becomes practically independent of Reynolds number. Similar trends can be observed from Fig. 7 for the bell-mouth inlet and were also observed for the square-edged inlet (see Ghajar and Augustine [18]).

Comparison of Figs. 6 and 7 for comparable Reynolds numbers shows that the length required for the apparent friction factor to become constant is shorter than what is required for the reentrant entrance. This could simply be attributed to the additional disturbance caused by this inlet.

PRACTICAL SIGNIFICANCE

The type of inlet configuration significantly influences the development of the friction factor along the pipe and the beginning and end of the transition region. The friction factor correlations provided in this study can be used to assist the heat exchanger designer in predicting the pressure drop along a horizontal straight circular tube for a specified inlet configuration.

SUMMARY AND CONCLUSIONS

This study provided an extensive and accurate pressure drop (friction factor) database across all flow regimes in the entrance and fully developed regions for a wide range of Reynolds numbers. The experimental friction factors in the fully developed laminar and turbulent flow regimes agreed within $\pm 5\%$ with the established correlations. The fully developed friction factor results for the inlet configurations used in this study showed that the range of Reynolds numbers

for which transition flow exists is 1980–2600 for the reentrant inlet, 2070–2840 for the square-edged inlet, and 2125–3200 for the bell-mouth inlet. Our experimentally obtained fully developed skin friction coefficients in the transition region for a bell-mouth entrance showed excellent agreement with Churchill's [14] correlation. Empirical correlations for the skin friction coefficient in the form of second-order polynomials were developed based on our fully developed data in the transition region for the reentrant, bell-mouth, and square-edged inlets.

Qualitative results are presented for the variation of laminar apparent friction along the entire length of the tube for different inlets. The results indicate that for low laminar Reynolds numbers the f_{app}(Re) factor is not just a function of $\mathrm{Re}/(x/D)$ as predicted by other investigators, but is a strong function of Reynolds number as well. The laminar apparent friction factor correlation of Shah [16] appears to apply to the bell-mouth inlet reasonably well for Reynolds numbers greater than 1500.

Support for this research was provided by the National Science Foundation under grant number CBT-88103342.

NOMENCLATURE

- c_f fully developed skin friction coefficient (fanning friction factor), $(= \Delta P D/2 L \rho V^2)$, dimensionless
- c_{fl} fully developed skin friction coefficient in the laminar flow regime, dimensionless
- c_{ft} fully developed skin friction coefficient in the turbulent flow regime, dimensionless
- $c_{f,\mathrm{tr}}$ fully developed skin friction coefficient in the transition flow regime, dimensionless
- D inside diameter of the test section, m
- f_{app} apparent Fanning friction factor $(= 2\Delta P_{0-x} D/x\rho V^2)$, dimensionless
- L length of test section, m
- Re Reynolds number $(= VD/\nu)$, dimensionless
- V average velocity in the test section, m/s
- x local axial distance along the test section from the inlet, m

Greek Symbols

- ΔP pressure difference, Pa
- ΔP_{0-x} pressure drop from the inlet to a specific location down the tube, Pa
- μ dynamic viscosity of test fluid, Pa · s
- ν kinematic viscosity of test fluid $(= \mu/\rho)$, m^2/s
- ρ density of test fluid, $\mathrm{kg/m}^3$

REFERENCES

1. Shah, R. K., and Johnson, R. S., Correlations for Fully Developed Turbulent Flow Through Circular and Noncircular Channels, Proc. Sixth National Heat and Mass Transfer Conf., Indian Inst. of Technology, Madras, India, pp. D-75–D-95, 1981.
2. Kakac, S., Shah, R. K., and Aung, W., *Handbook of Single-Phase Convective Heat Transfer*, Wiley, New York, 1987.
3. Ghajar, A. J., Strickland, D. T., and Kuppuraju, S., Forced and Mixed Convective Heat Transfer Measurements in a Circular Tube with Different Inlets, in *Mixed Convection*, R. L. Mahajan and R. D. Boyd, Eds., HTD-Vol. 152, pp. 37–45, ASME, New York, 1990.
4. Ghajar, A. J., and Tam, L. M., Laminar-Transition-Turbulent Forced and Mixed Convective Heat Transfer Correlations for Pipe Flows with Different Inlet Configurations, in *Fundamentals of Heat Transfer in Forced Convection*, Proceedings of the 1991 ASME Winter Annual Meeting (in Press).
5. Kong, S. C., Intermittency Factor Measurements in the Transition Region for a Circular Tube with Square-Edged and Re-entrant Entrances, M.S. Report, Oklahoma State Univ., School of Mechanical and Aerospace Engineering, Stillwater, 1990.
6. Augustine, J. R., Pressure Drop Measurements in the Transition Region for a Circular Tube with a Square-Edged Entrance, M.S. Thesis, Oklahoma State Univ., Stillwater, 1990.
7. Morel, T., Comprehensive Design of Axisymmetric Wind Tunnel Contractions, *Trans. ASME J. Fluids Eng.*, **97**, 225–223, 1975.
8. Bohn, D., Fischer, S., and Obermeir, E., Thermal Conductivity, Density, Viscosity, and Prandtl Numbers of Ethylene Glycol–Water Mixtures, *Ber. Bunsenges. Phys. Chem.*, **88**, 739–742, 1984.
9. Ghajar, A. J., and Zurigat, Y. H., Microcomputer-Assisted Heat Transfer/Analysis in a Circular Tube, *J. Appl. Eng. Educ.*, 7(2), 125–134, 1991.
10. Blasius, H., Das Ähnlichkeitsgesetz bei Reibungsvorgängen in Flüssigkeiten, *Forsch. Arb. Ing.-Wes.*, 131, 1913.
11. Kline, S. J., and McClintock, F. A., Describing Uncertainties in Single Sample Experiments, *Mech. Eng.*, 75(1), 3–8, 1953.
12. Madon, K. F., Pressure Drop Measurements in the Transition Region for a Circular Tube with a Re-Entrant and Bell-Mouth Entrance, M.S. Report, Oklahoma State Univ., School of Mechanical and Aerospace Engineering, Stillwater, 1990.
13. Hrycak, P., and Andruskhiw, R., Calculation of Critical Reynolds Number in Round Pipes and Infinite Channels and Heat Transfer in Transition Regions, *Heat Transfer 1974*, **2**, 183–187, 1974.
14. Churchill, S. W., Comprehensive Correlating Equations for Heat, Mass and Momentum Transfer in Fully Developed Flow in Smooth Tubes, *Ind. Eng. Chem. Fundam.*, **16**, 109–116, 1977.
15. Bhatti, M. S., and Shah, R. K., Turbulent and Transition Flow Convective Heat Transfer in Ducts, in *Handbook of Single-Phase Convective Heat Transfer*, S. Kakac, R. K. Shah, and W. Aung, Eds., Chapter 4, p. 16, Wiley, New York, 1987.
16. Shah, R. K., A Correlation for Laminar Hydrodynamic Entry Length Solutions for Circular and Noncircular Ducts, *J. Fluids Eng.*, **100**, 177–179, 1978.
17. Langhaar, H. L., Steady Flow in the Transition Length of a Straight Tube, *J. Appl. Mech.*, **9**, A-55–A-58, 1942.
18. Ghajar, A. J., and Augustine, J. R., Pressure Drop Measurements in the Transition Region for a Circular Tube with a Square-Edged Entrance, Presented at the AIAA 21st Fluid Dynamics, Plasma Dynamics and Lasers Conference, Seattle, AIAA Paper No. 90-1500, 1990.

Received February 20, 1991; revised September 16, 1991